Journal of Medicinal Chemistry

Article

pubs.acs.org/jmc

Revisiting [$PtCl_2$(*cis*-1,4-DACH)]: An Underestimated Antitumor Drug with Potential Application to the Treatment of Oxaliplatin-Refractory Colorectal Cancer

Nicola Margiotta,*[,†] Cristina Marzano,[‡] Valentina Gandin,[‡] Domenico Osella,[§] Mauro Ravera,[§] Elisabetta Gabano,[§] James A. Platts,[∥] Emanuele Petruzzella,[†] James D. Hoeschele,[⊥] and Giovanni Natile*[,†]

[†]Dipartimento Farmaco-Chimico, Università di Bari "A. Moro", via E. Orabona 4, 70125 Bari, Italy

[‡]Dipartimento di Scienze del Farmaco, Università di Padova, via Marzolo 5, 35131 Padova, Italy

[§]Dipartimento di Scienze e Innovazione Tecnologica, Università del Piemonte Orientale "A. Avogadro", viale T. Michel 11, 15121 Alessandria, Italy

[∥]School of Chemistry, Cardiff University, Park Place, Cardiff CF10 3AT, United Kingdom

[⊥]Department of Chemistry, Eastern Michigan University, Ypsilanti, Michigan 48197, United States

Supporting Information

ABSTRACT: Although the encouraging antitumor activity of [$PtCl_2$(*cis*-1,4-DACH)] (**1**; DACH = diaminocyclohexane) was shown in early studies almost 20 years ago, the compound has remained nearly neglected. In contrast, oxaliplatin, containing the isomeric 1(*R*),2(*R*)-DACH carrier ligand, enjoys worldwide clinic application as a most important therapeutic agent in the treatment of colorectal cancer. By extending the investigation to human chemotherapy-resistant cancer cells, we have demonstrated the real effectiveness of **1** in circumventing cisplatin and oxaliplatin resistance in LoVo colon cancer cells. The uptake of compound **1** by the latter cells was similar to that of sensitive LoVo cells. This is not the case for all other compounds considered in this investigation. Interaction with double-stranded DNA, investigated by a biosensor assay and by quantum mechanical/molecular mechanical geometry optimization of the 1,2-GG intrastrand cross-link, does not show significant differences between **1** and oxaliplatin. However, the DNA adducts of **1** are removed from repair systems with lower efficiency and are more effective in inhibiting DNA and RNA polymerase.

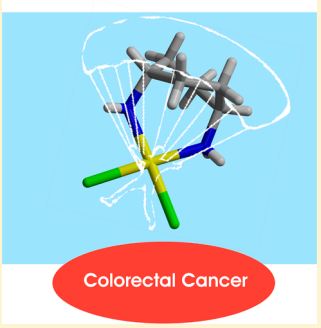

INTRODUCTION

Platinum drugs (cisplatin, *cis*-diamminedichloridoplatinum(II) (CDDP), carboplatin, diammine[1,1-cyclobutanedicarboxylato]platinum(II), and oxaliplatin, [1(*R*),2(*R*)-cyclohexane-1,2-diamine](ethanedioato)platinum(II); Figure 1) are widely used in the clinic, and the prototype cisplatin still represents the only antineoplastic drug with highly curative effects in a solid malignancy such as testicular cancer.[1−7] The complex [$PtCl_2$(*cis*-1,4-DACH)] (DACH = diaminocyclohexane), **1**, contains an isomeric form of the oxaliplatin diamine ligand and has been widely investigated as a potential new platinum anticancer drug.

The first paper reporting the in vitro and in vivo activities of **1** was published by one of us.[8] The in vitro growth inhibition data indicated that **1** exhibited potent activity in sensitive L1210 and P388 cell lines and that the compound also appeared more potent than cisplatin (on the basis of ID_{50} values) against all tested Pt-resistant cell lines, with the only exception the cisplatin-resistant cell lines L1210PtR4 and L1210DDP5 (partial cross-resistance) and the oxaliplatin-resistant cell line L1210DACH. In vivo, **1** proved to be more dose potent than cisplatin (on the basis of T/C (%) values) against the parental L1210 and P388 murine leukemias. Compound **1** also retained a significant activity against sublines derived from L1210 and P388 and made resistant to cisplatin. Both **1** and cisplatin produced equivalent activity against B16 melanoma and M5076 sarcoma, while cisplatin was more active than **1** against colon carcinoma 26 at equitoxic doses. These initial data suggested that the spectrum of activity of **1** could have been different from those of cisplatin and oxaliplatin.

Two years later, the group of Khokhar reported the in vitro cytotoxicity of **1** against murine leukemia L1210 and human ovarian cancer A2780 cells.[9] The compound was found to be more active than cisplatin and tetraplatin ($Pt^{IV}Cl_4$(1(*R*),2(*R*)-DACH)) in both cell lines (the human A2780 cell line being more sensitive). The high potency and the high solubility in water of **1** made this compound an ideal lead for further studies. Khokhar and collaborators also explored Pt^{IV}(*cis*-l,4-DACH) derivatives[10] and found that, among a series of complexes having the general formula *cis,cis,trans*-[$Pt^{IV}Cl_2$(*cis*-1,4-DACH)-L_2] (L = $CH_3(CH_2)_nCOO-$, *n* = 0−8), *cis,cis,trans*-[$Pt^{IV}Cl_2$(*cis*-1,4-DACH)$(CH_3COO)_2$] was the most active in the murine L1210 leukemia model. Khokhar and colleagues also prepared

Received: May 16, 2012
Published: July 12, 2012

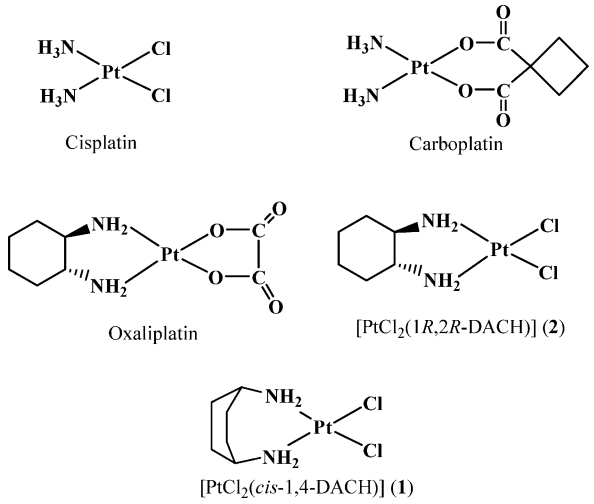

Figure 1. Sketches of cisplatin, carboplatin, oxaliplatin, [$PtCl_2$(1(*R*),2-(*R*)-DACH)] (**2**), and [$PtCl_2$(*cis*-1,4-DACH)] (**1**).

and characterized monofunctional[11] and bifunctional[12] adducts of **1** with nucleobases as models for DNA binding of these Pt antitumor drugs.[13,14]

A peculiar feature of platinum-coordinated *cis*-1,4-DACH is the formation of a seven-membered chelate ring, which is larger than the usually encountered five- and six-membered rings (X-ray diffraction data).[15] This results in a very large bite angle (≥97°) that could affect the mobility of *cis* ligands. Indeed, some of us investigated the (*cis*-1,4-DACH)PtG_2 system (G = two untethered guanine bases) and,[15] by lowering the temperature, were able to observe the presence of different rotamers in solution (two HT, head-to-tail, conformers and one HH, head-to-head, conformer are possible in aqueous solution).[16]

The unique antitumor activity of **1** was further investigated with reference to cell entry, reaction with sulfur-containing compounds, binding to DNA, and processing of DNA adducts by proteins (including DNA repair enzymes).[17] In particular, compared to cisplatin, **1** revealed (i) improved cytotoxicity (3.4−5.4-fold greater) and enhanced cellular uptake (ca. 1.5-fold greater) in the human ovarian A2780 cancer cell line, (ii) an enhanced rate but similar sequence preference for DNA binding in cell-free media, (iii) an identical DNA interstrand cross-linking efficiency (6%), (iv) similar bending (32°) but enhanced local DNA unwinding (ca. 1.5-fold greater) for 1,2-GG intrastrand cross-links, and (v) markedly enhanced inhibition of DNA polymerase accompanied by significantly lower efficiency of DNA repair.

Colorectal cancer is at the top of the list of the most common cancers worldwide, with around 1 million new cases diagnosed every year.[18] Early-stage colorectal cancer is frequently curable with surgery, but the appearance of metastases leads to unresectable tissues with fatal consequences for the patient.[19] The best outcome in the therapy of metastatic colorectal cancer is obtained by the use of 5-fluorouracil, oxaliplatin, and irinotecan. More recently, biological therapies have also proved to be effective in prolonging the median survival time.[20]

Presently, apart from oxaliplatin, there are no other drugs in advanced clinical development which appear to be active against colorectal cancer and that could be used for the treatment of patients with oxaliplatin-refractory colorectal cancer. This prompted us to test compound **1** against human colorectal cancer cells and, in particular, colorectal cancer cells resistant to oxaliplatin. Furthermore, since inhibition of DNA polymerase by Pt(*cis*-1,4-DACH)−DNA adducts appears to be markedly different from that of cisplatin−DNA adducts, although both compounds give similar intrastrand (and interstrand) DNA cross-links,[21,22] we explored the interaction of **1** with double-stranded (ds) DNA using an electrochemical biosensor and computational methods.

RESULTS AND DISCUSSION

Cytotoxicity. Compound **1** was prepared for the first time almost 20 years ago; however, until now, it had been tested (both in vitro and in vivo) only in a limited number of tumor cell lines.[8,9] To extend the pharmacological investigation, two Pt(II) complexes containing isomeric forms of diaminocyclohexane, [$PtCl_2$(*cis*-1,4-DACH)] (**1**) and [$PtCl_2$(1(*R*),2(*R*)-DACH)] (**2**), have been evaluated for their cytotoxic activity toward a panel of human tumor cell lines, including cervical (A431), breast (MCF-7), and colon (HCT-15) cancers along with a melanoma (A375). The cytotoxicity was evaluated by means of the 3-(4,5-dimethylthiazol-2-yl)-2,5-diphenyltetrazolium bromide (MTT) test for 72 h treatment with increasing concentrations of the tested compounds. For comparison purposes, the cytotoxicities of cisplatin, the most widely used anticancer metallodrug, and oxaliplatin, a key drug in FOLFOX (folinic acid, 5-fluorouracil, and oxaliplatin) regimens for the treatment of colorectal cancers, were evaluated in the same experimental conditions. IC_{50} values, calculated from dose−survival curves, are reported in Table 1.

Compound **1** was found, on average, slightly more effective than oxaliplatin, much more effective than cisplatin (by a factor of 3−6) in two out of the four cell lines (HCT-15 and MCF-7, characterized for their scarce sensitivity to cisplatin), and, on average, 2−4 times more active than compound **2**, which has the same diamine of oxaliplatin but chloride leaving ligands like **1**.

The four compounds have been additionally tested for their in vitro antitumor activity in two pairs of human cell lines which

Table 1. In Vitro Antitumor Activity[a]

	IC_{50} (μM) ± SD			
compound	HCT-15	MCF-7	A375	A431
1	2.66 ± 0.95	3.09 ± 1.06	1.87 ± 1.25	1.46 ± 0.91
2	8.02 ± 1.84	9.52 ± 2.36	6.14 ± 1.45	6.69 ± 3.27
oxaliplatin	1.25 ± 1.05	3.36 ± 1.69	2.37 ± 1.31	3.69 ± 1.03
cisplatin	15.53 ± 2.48	8.37 ± 2.96	2.06 ± 1.01	1.96 ± 0.84

[a]Cells ((3−8) × 10^4 mL^{-1}) were treated for 72 h with increasing concentrations of tested compounds. Cytotoxicity was assessed by the MTT test. IC_{50} values were calculated by the four-parameter logistic model ($p < 0.05$). SD = standard deviation.

dx.doi.org/10.1021/jm3006838 | J. Med. Chem. 2012, 55, 7182−7192

Table 2. Cross-Resistance Profiles[a]

	IC_{50} (μM) ± SD				
compound	2008	C13*	LoVo	LoVo-OXP	LoVo MDR
1	1.89 ± 1.04	1.77 ± 0.92 (0.9)	1.11 ± 0.45	1.29 ± 0.82 (1.2)	1.09 ± 0.46 (1.0)
2	8.57 ± 2.03	17.06 ± 1.35 (2.0)	5.62 ± 0.94	14.64 ± 1.84 (2.6)	5.07 ± 0.82 (0.9)
oxaliplatin	1.65 ± 1.01	3.33 ± 1.84 (2.0)	1.02 ± 0.56	17.50 ± 1.79 (17.0)	1.36 ± 0.81 (1.3)
cisplatin	2.26 ± 1.06	23.73 ± 2.42 (10.5)	7.63 ± 1.53	13.13 ± 2.47 (1.7)	7.53 ± 0.98 (1.1)

[a]Cells ((3−8) × 10^4 mL^{-1}) were treated for 72 h with increasing concentrations of tested compounds. Cytotoxicity was assessed by the MTT test. IC_{50} values were calculated by the four-parameter logistic model ($p < 0.05$). SD = standard deviation. The resistance factor (RF = IC_{50}(resistant)/IC_{50}(parent line)) is given in parentheses.

have been selected for their resistance to cisplatin (ovarian cancer cells 2008/C13*) or oxaliplatin (colon cancer cells LoVo/LoVo-OXP). A LoVo cell line retaining a multi-drug-resistance phenotype was also considered (LoVo MDR). Cross-resistance profiles were evaluated by means of the resistance factor (RF), which is defined as the ratio between the IC_{50} value for the resistant cells and that arising from the sensitive cells (Table 2).

Cisplatin resistance is multifactorial in nature; however, the main molecular mechanisms involved in drug resistance of C13* cancer cells have been identified in high cellular glutathione and thioredoxin reductase levels, in reduced cellular drug uptake, and in enhanced repair of DNA damage. The molecular mechanisms involved in oxaliplatin resistance have not been so well characterized; however, they appear to be (i) decreased cellular accumulation, which is thought to be related to a greater activity of the ATP7B exporter rather than to the activity of P-glycoprotein (P-gp) and multi-drug-resistance protein 1 (MRP1), and (ii) more efficient repair of oxaliplatin-induced DNA damage by NER (nucleotide excision repair).[23−26]

It is noteworthy that, although oxaliplatin induces the same type of DNA cross-links as cisplatin, it is effective also in cell lines resistant to cisplatin, thus suggesting that the two complexes may have different mechanisms of resistance.[27] LoVo-OXP cells (derived from LoVo cells grown in the presence of increased concentrations of oxaliplatin) were 17-fold more resistant than parental cells (see Table 2). The data reported in Table 2 clearly indicate that compound **1** is as good as oxaliplatin and better than cisplatin (particularly in the case of colon cancer cells) toward the sensitive lines. Moreover, compound **1** does not show cross-resistance to cisplatin (RF = 0.9) nor to oxaliplatin (RF = 1.2). On the other hand, oxaliplatin is partially cross-resistant to cisplatin (RF = 2.0) and cisplatin partially cross-resistant to oxaliplatin (RF = 1.7). Compound **2**, which has the same diamine as oxaliplatin but two leaving chlorides like cisplatin and compound **1**, is, on average, 5−10 times less effective than compound **1** and exhibits partial cross-resistance to both cisplatin (RF = 2.0) and oxaliplatin (RF = 2.6).

These findings are in agreement with those previously reported for human ovarian 2780/2780R cancer cells[17] and for murine leukemia [$PtCl_2$(1,2-DACH)]-resistant cells.[8] Therefore, it is possible to conclude that in human colorectal cancer cells **1** is not recognized as a Pt(DACH) complex, confirming that differences in the shape of the diamine ligand can play a key role in the antitumor effect of Pt(DACH) complexes.

In Table 2 are also reported the results obtained in a multi-drug-resistant (MDR) colon carcinoma subline, LoVo MDR, in which the resistance to doxorubicin, a drug belonging to the MDR spectrum, is associated with an overexpression of multispecific drug transporters, such as the 170 kDa P-gp.[28] It is well-known that acquired MDR, whereby cells become refractory to multiple drugs, poses a most important challenge to the success of anticancer chemotherapy. Although cisplatin is not a P-glycoprotein substrate, many multi-drug-resistance proteins (MRP1, MRP2, MRP4) have been claimed to be involved in platinum complex transport and to be responsible for its afflux to/efflux from the cell.[23−25] All platinum derivatives tested against this cell line showed a response similar to that for the parental subline, thus suggesting that platinum drugs are not P-gp substrates.

Cellular Uptake and Lipophilicity. It is well-known that cellular uptake is an important factor influencing drug efficacy. Moreover, since one of the main mechanisms controlling oxaliplatin resistance is cellular uptake, uptake experiments were performed in human colorectal cancer cells sensitive and resistant to oxaliplatin. Cancer cells were treated for 6, 24, and 48 h with 5 μM concentrations of **1**, **2**, and oxaliplatin. The intracellular platinum was quantified by means of GF-AAS analysis, and the results, expressed as μg of metal mg^{-1} of cellular proteins, are summarized in Figure 2.

The platinum cellular uptake was time dependent for all platinum complexes and for sensitive as well as for resistant LoVo cells (Figure 2). There is, however, a marked difference between sensitive and resistant cells as far as the discrimination between different complexes is concerned. In LoVo sensitive cells the amount of incorporated drug is practically the same for the three types of complexes, clearly indicating that the smaller activity of compound **2** in this colon tumor cell line is to be ascribed to factors other than cellular drug uptake. In resistant LoVo-OXP cells (Figure 2B) the cellular uptake is remarkably decreased for oxaliplatin and compound **2** (both compounds having the 1,2-DACH ligand) but not for compound **1**, which is internalized with the same efficacy in LoVo as well as in LoVo-OXP cells. These data can well explain the lack of cross-resistance between compound **1** and oxaliplatin. It is also to be noted that while for compound **2** the observed RF (2.6) can be accounted for by the reduced cellular uptake, in the case of oxaliplatin the observed RF (17.0) is far too great to be justified only on the basis of differential cellular uptake.

The main differences between cisplatin and oxaliplatin are distribution in the body, cellular accumulation, and recognition and processing of DNA adducts. These differences are ascribable, at least in part, to the presence of the organic diamine ligand in oxaliplatin, which confers lipophilicity and steric bulk. On this basis, other groups have pursued the preparation of platinum derivatives having the methyl-substituted 1(*R*),2(*R*)-DACH ligand with the aim of improving the cytotoxic and anticancer properties of the drug by increasing its lipophilicity and steric bulk.[29]

dx.doi.org/10.1021/jm3006838 | J. Med. Chem. 2012, 55, 7182−7192

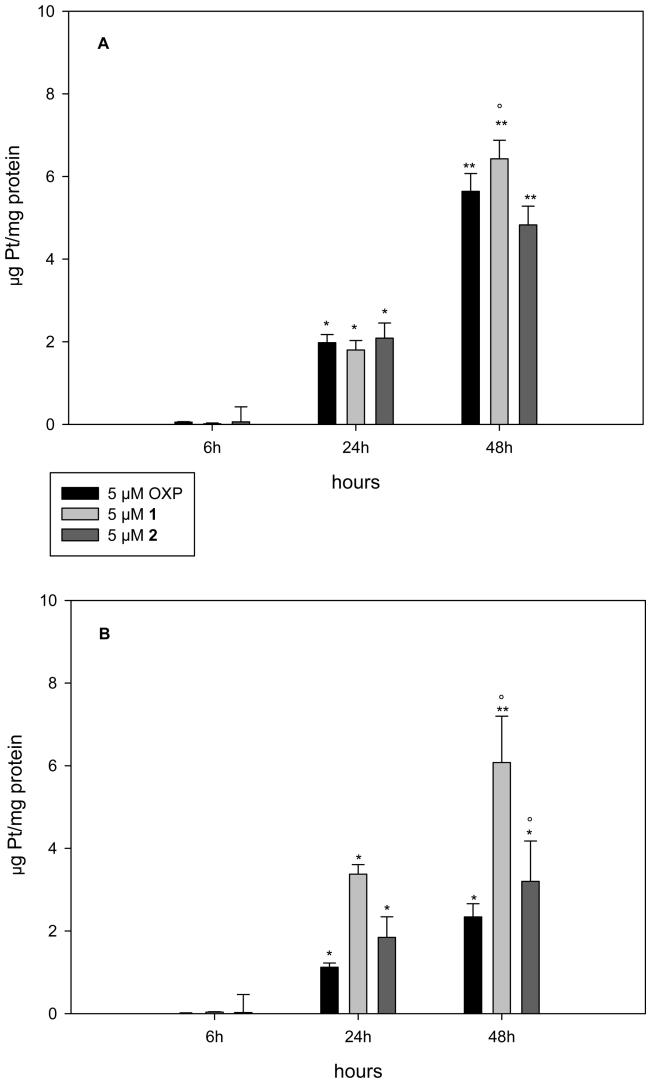

Figure 2. Intracellular accumulation of platinum complexes detected by GF-AAS analysis. LoVo (A) and LoVo-OXP (B) cells were incubated with 5 μM concentrations of complexes **1** and **2** and oxaliplatin (OXP) for 6, 24, and 48 h. Error bars indicate the standard deviation. Key: *, $p < 0.05$; **, $p < 0.01$ compared to the control, ○, $p < 0.05$ compared to oxaliplatin-treated cells.

It is generally found that the cellular uptake of platinum complexes correlates with their lipophilicities.[30,31] Lipophilicity is usually expressed in terms of the 1-octanol/water partition coefficient, log $P_{o/w}$, and correlates with cellular uptake by passive diffusion.[32] Since RP-HPLC retention is due to partitioning between mobile (polar) and stationary (apolar) phases, there is a good correlation between the capacity factor k' ($k' = (t_R - t_0)/t_0$, where t_0 is the retention time for an unretained compound and t_R is the retention time of the analyte) and partition coefficient (log $P_{o/w} = a + b \log k'$). Thus, the HPLC procedure represents a good alternative to the time- and material-consuming shake-flask method. By using the HPLC procedure, log $P_{o/w}$ of compound **1** was found to be -1.57 ± 0.10, in good agreement with that of compound **2** (log $P_{o/w} = -1.40$) or oxaliplatin (log $P_{o/w} = -1.39$)[33] but significantly greater than that of cisplatin (log $P_{o/w} = -2.27$) or [$PtCl_2$(en)] (log $P_{o/w} = -2.16$; en = ethylenediamine). Thus, the intracellular platinum accumulation exhibited by **1**, **2**, and oxaliplatin in sensitive LoVo cells (Figure 2A) appears to be strictly related to their very similar log $P_{o/w}$ values, which could imply that the three complexes enter the cells by a similar route and this could be (but not exclusively) passive diffusion. On the contrary, in the case of oxaliplatin-resistant LoVo-OXP cells, the cellular accumulation decreases remarkably for compound **2** and oxaliplatin (containing the 1,2-DACH ligand) but not for compound **1** (containing *cis*-1,4-DACH). This implies that there are specific import (CTR1, OCT, etc.) or export (ATP7B) mechanisms which operate selectively on the different types of complexes.

In Vivo Antitumor Activity in Lewis Lung Carcinoma. The in vivo antitumor activity of **1** was evaluated in a model of solid tumor, the syngeneic murine Lewis lung carcinoma (LLC). Tumor growth inhibition induced by **1** was compared with that promoted by the reference metallodrug cisplatin. From day 9 after tumor inoculation, when tumors became palpable, tumor-bearing mice received daily doses of **1** (1.5 and 3 mg kg^{-1}) or cisplatin (1.5 mg kg^{-1}). Tumor growth was estimated at day 15, and the results are summarized in Table 3. For the assessment of the adverse side effects, changes in the body weights of tumor-bearing mice were daily monitored (Figure 3).

Table 3. In Vivo Anticancer Activity toward Murine Lewis Lung Carcinoma[a]

	daily dose ip (mg kg^{-1})	av tumor wt (mean ± SD, g)	inhibition of tumor growth (%)
control[b]		0.778 ± 0.05	
1	1.5	0.253 ± 0.09**	67.48
1	3	0.158 ± 0.06**	79.69
cisplatin	1.5	0.199 ± 0.10**	74.66

[a]Starting from day 9 after tumor implantation, tested compounds were daily administered intraperitoneally (ip). At day 15, mice were sacrificed, and tumor growth was detected as described in the Experimental Section. Tukey–Kramer test: **, $p < 0.01$. [b]Vehicle (0.9% NaCl).

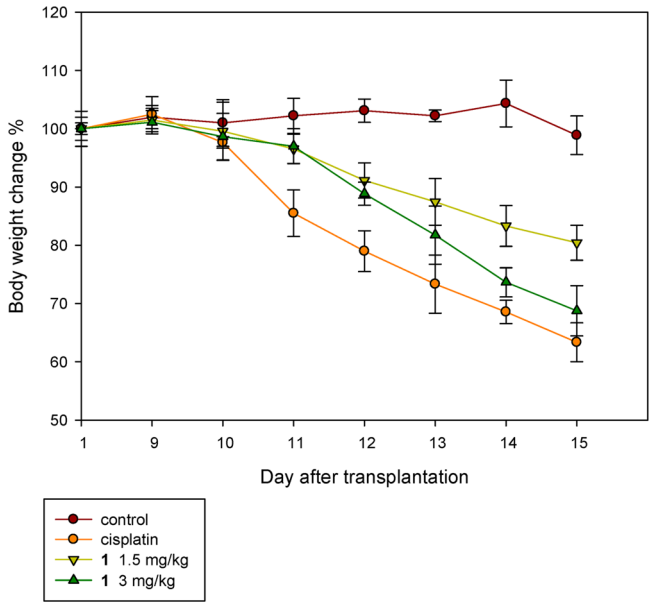

Figure 3. Body weight changes of LLC-bearing C57BL mice treated with vehicle or tested compounds. Each drug was administered daily from day 9, and the weights were detected at day 1 and daily from day 9. The error bars indicate the SD.

dx.doi.org/10.1021/jm3006838 | J. Med. Chem. 2012, 55, 7182–7192

Compound **1** is better tolerated than cisplatin and could be administered also at a greater dose (3 mg kg^{-1}). The inhibition of tumor cell proliferation for the three compounds is reported in Table 3. Even at the lower daily dose of 1.5 mg kg^{-1}, compound **1** exerts a statistically significant ($p < 0.01$) antitumor activity, with a tumor growth inhibition of 67%. A reduction (about 80%) of the tumor volume was achieved using a daily dose of 3.0 mg kg^{-1}. The antitumor activity of cisplatin (73%) is between those obtained with compound **1** at the two different doses. It is however remarkable that the body weight loss (depicted in Figure 3) indicates that, even at the higher dose (3 mg kg^{-1}), compound **1** had smaller adverse side effects than cisplatin and that, at equimolar dose (1.5 mg kg^{-1}), the weight loss caused by compound **1** is about half that caused by cisplatin.

Interaction with DNA. In the last part of this work we look to possible differences between compounds **1** and **2** (the latter similar to oxaliplatin except for the leaving ligands, two chlorides, which are similar to those of **1**) in their interaction with DNA. The two compounds exhibit remarkably different toxicities toward tumor cells (on the average 5 times greater for **1** with respect to **2**). Moreover, while **1** is not cross-resistant to cisplatin or oxaliplatin, **2** is. **1** and **2** have been shown to have similar lipophilicities and similar uptakes by sensitive tumor cells; however, their uptakes by resistant cells are different. The two compounds could also have different reactivities toward DNA or give different distortions as, for example, is the case for compounds of type **2** with different configurations of the diamine (either (*R*,*R*)- or (*S*,*S*)-1,2-DACH).

Rate of Reaction with Double-Stranded DNA. The rate of reaction with DNA has been investigated using an electrochemical biosensor, while investigation of different distortions of the DNA adduct has been attempted by computational methods.

Briefly, an electrochemical biosensor may be produced by immobilization of ds-DNA on the surface of a screen-printed electrode (SPE), and square wave voltammetry (SWV) can be exploited to measure the oxidation peak of guanines.[34] Any agent reacting with guanines and causing a decrease in their electron density will also cause a decrease of their oxidation peak current.[35−39] Thus, the interaction between the complex and DNA can be evaluated as the decrease (*S*, %) of the guanine oxidation peak height for the electrode immersed in the drug solution or in the buffer solution without drug.

Figure 4 shows the binding of **1**, **2**, and cisplatin, evaluated as *S* (%), vs interaction time. Both compounds show very similar *S* vs time curves, indicating a substantial similarity in the rate of interaction with ds-DNA. Moreover, at a given time point *S* values are higher for compounds **1** and **2** than for cisplatin, revealing a lower rate of interaction of the former compounds with DNA. Such a lower reactivity could well depend upon the greater steric bulk of the carrier ligands.

The solvolysis kinetics for the two compounds could be checked directly by measuring the conductivity of **1** and **2** in pure DMSO solution. Figure 5 shows the changes, as a function of time, of the conductivity of 0.5 mM solutions of **1** and **2** in DMSO at 25 °C. In DMSO the original neutral species $[PtA_2Cl_2]$ (A_2 = diamine ligand) is converted into a 1:1 electrolyte, $[PtA_2Cl(DMSO)]^+$ and Cl^-.

For a solvolysis time >700 min, the conductivity Λ of both complexes reaches a plateau at a value of ca. 15 μS. This is in accord with a 1:1 electrolyte which, in such a solvent, usually exhibits a millimolar conductivity between 20 and 50 μS (i.e., 10−25 μS for a 0.5 mM solution).[40] The conductivity data were processed to obtain the pseudo-first-order rate constant *k* (the Guggenheim plot of $\ln|\Lambda_t - \Lambda_{t+\Delta}|$ vs *t* affords a linear relationship having slope *k*).[41] The calculated rate constants are 6.63×10^{-3} and 3.85×10^{-3} min^{-1} for **1** and **2**, respectively (corresponding to $t_{1/2}$ values of 104 and 180 min, respectively).

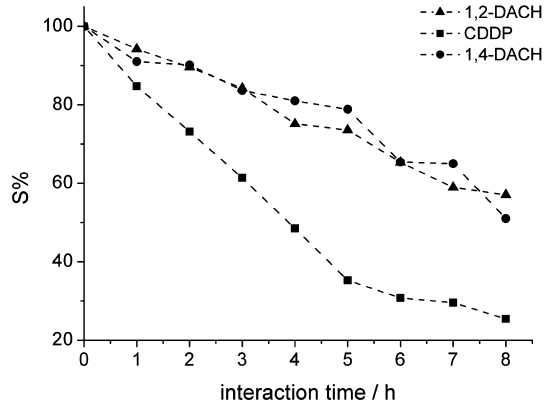

Figure 4. *S* (%) vs interaction time for a 0.25 mM solution of **1** (circles), **2** (triangles), or cisplatin (squares) interacting with ds-DNA in 50 mM PBS + 5 mM NaCl and 2% DMSO, pH 7.4. Each time point is the mean of three independent experiments (standard deviation ≤10%). The electrochemical conditions are given in the Experimental Section.

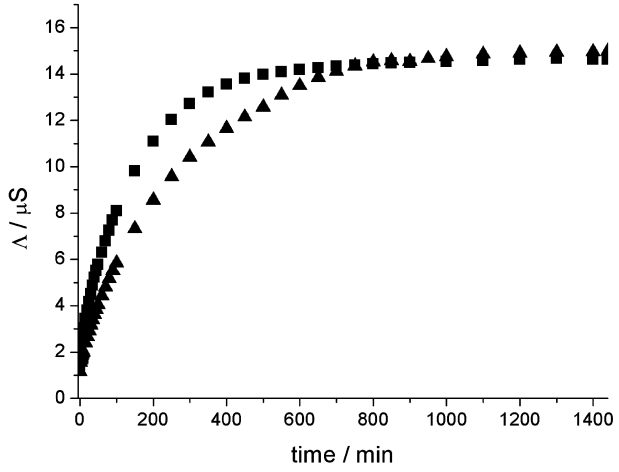

Figure 5. Conductivity against time for 0.5 mM solutions of **1** (triangles) and **2** (squares) in DMSO at 25 °C.

Modeling of the 1,2-GG Cross-Link. To investigate possible structural differences between DNA adducts of **1** and **2**, we performed QM/MM geometry optimization of the 1,2-GG intrastrand cross-links. Figure 6 shows the optimized geometries of the two adducts and also illustrates the employed partition into QM and MM regions. In both adducts, the pairing between G and C bases is distorted but essentially preserved.

In the DNA adduct of **1**, the 1,4-DACH cyclohexyl ring adopts a twist-boat conformation, and a hydrogen bond between a coordinated amine and O6 of 3′-G (H···O distance 1.751 Å) is formed. The geometrical requirements of the ligand and DNA backbone require that the other O6 cannot form a similar hydrogen bond (closest H···O distance 3.119 Å). In the adduct of **2**, the 1,2-DACH cyclohexyl ring adopts a chair conformation, and a similar hydrogen-bonding pattern, with

dx.doi.org/10.1021/jm3006838 | J. Med. Chem. 2012, 55, 7182−7192

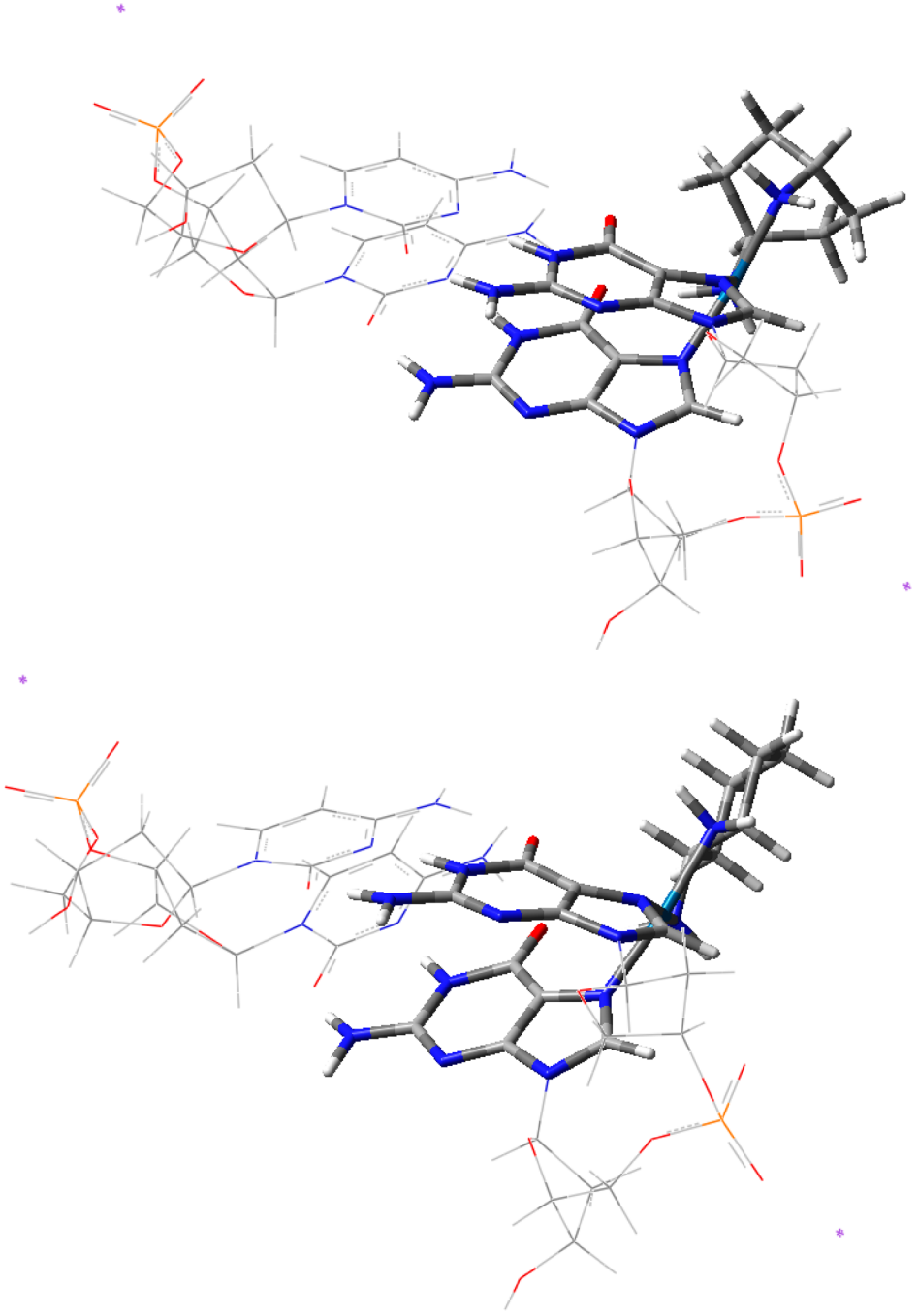

Figure 6. Optimized geometries for the adducts of **1** (top) and **2** (bottom) with a GG/CC base-pair step. Atoms included in the QM region are shown as solid, while those included in the MM region are shown as wireframe.

H···O6 distances of 1.732 and 3.183 Å for 3′-G and 5′-G, respectively, is found. These hydrogen bond distances are considerably shorter than those observed by Chaney in the NMR solution structure of the adduct of oxaliplatin with a DNA dodecamer (2.85 and 3.93 Å),[42] thus reflecting the greater flexibility of the smaller DNA fragment employed in our calculations. A hydrogen bond between an aminic group of 1,2-DACH and O6 of 3′-G was also observed by Lippard in the X-ray structure of a ds-dodecamer containing a unique oxaliplatin−GG adduct.[43] Also in that case the N···O6 distance (2.9 Å) was greater than that observed in our model (N···O6 distances of 2.76 and 2.69 Å for the adducts of **1** and **2**, respectively).

Table 4 reports the binding energies evaluated for the optimized QM/MM geometries. The employed BHandH method is known to overestimate the metal−DNA binding energy,[44] so we also evaluated the binding energies using the more reliable B97-D density functional theory (DFT) method,

Table 4. Binding Energies for Compounds 1 and 2 and Cisplatin, Corrected for Solvation Effects (kcal mol^{-1})

	1	2	cisplatin
QM/MM	−136.1	−147.4	−133.0
DFT	−106.6	−109.2	−110.5
PM6-DH2	−108.4	−112.7	−106.9

dx.doi.org/10.1021/jm3006838 | *J. Med. Chem.* 2012, 55, 7182−7192

along with the much faster PM6-DH2 semiempirical approach. Analogous data for cisplatin are also included for comparison. All three complexes are found to be strongly bound to the DNA due to the large electrostatic attraction between the positively charged platinum fragment and the nucleophilic DNA. On the average, compound **2** appears to be the most strongly bound, whereas **1** shows a binding energy similar to that of cisplatin.

The distortion of the GG/CC base-pair step is analyzed in Table 5. For comparison, the same parameters obtained for the unplatinated fragment and for the cisplatin−GG/CC adduct, both optimized at the same level, are also included. All platinum adducts show significant distortion from free DNA, but the magnitude and sign of these distortions are different for the adducts of compounds **1** and **2**. Data for the entire base-pair step indicate that **1** behaves like cisplatin more than does **2**. For instance, **1** and cisplatin show large changes in shift, slide, and rise from free DNA, whereas **2** has values of these parameters much closer to those of undamaged DNA. All structures exhibit negative tilt values and large, positive values of roll; only the twist parameter in the adduct of **1** is significantly different from all others. **1** and cisplatin also exhibit similar stretch and stagger values for individual base pairs, which are quite different from those of **2**.

Table 5. X3DNA Analysis for Compounds 1 and 2, Cisplatin, and B-DNA

	1	2	cisplatin	B-DNA[a]
shift	+1.19	+0.95	+1.10	+0.87
slide	−1.39	−1.60	−1.31	−1.73
rise	+2.85	+3.34	+2.99	+3.83
tilt	−7.90	−5.50	−5.27	+2.27
roll	+16.13	+25.51	+14.71	−1.02
twist	+19.73	+23.88	+24.41	+36.16
shear	−0.77	−0.63	−0.68	−0.02
	−0.44	−0.51	−0.31	
stretch	−0.34	−0.28	−0.34	+0.14
	−0.17	−0.22	−0.18	
stagger	−0.20	−0.11	−0.26	+0.02
	+0.03	−0.11	+0.06	
buckle	+4.40	+16.63	−3.27	+14.25
	+14.93	+8.87	−1.25	
propeller	−6.78	−10.07	−18.85	−7.79
	+5.99	−2.18	−3.18	
opening	+0.24	+0.23	+0.34	+4.41
	+1.22	+1.63	−0.24	

[a]Optimized at the same QM/MM method.

Processing of the DNA Lesions. The absence of significant differences in the rate of reaction of **1** and **2** with ds-DNA and in the conformations of the GG cross-links, as outlined in the previous paragraphs, is in accord with the results of a previous work reported by some of us in which it was shown that the DNA binding mode of **1** (sequence preference, type of major adduct, and resulting conformational alterations) is not very different from that of cisplatin.[17] However, some significant differences were found in the processing of the DNA lesions. In particular, in cell-free extracts as well as in living cells, the 1,2-GG cross-links of **1** were removed from DNA by DNA repair systems with a slightly lower efficiency than adducts of cisplatin. As a consequence, the adducts of **1** may persist somewhat longer on DNA than the adducts of cisplatin, potentiating the antitumor activity of **1**. Moreover, the 1,2-GG intrastrand cross-links formed by **1** inhibited DNA polymerase more efficiently than the analogous adducts formed by cisplatin, so that they can be bypassed by DNA polymerases with greater difficulty.[17] This latter effect could increase the sensitivity of tumor cells to **1** as a consequence of a lowered adduct tolerance mediated by the reduced ability of DNA polymerases to replicate past platinum adducts. Since the conformational distortions induced in DNA by compound **1** and cisplatin are similar but their cellular processing is different,[45] the greater size of *cis*-1,4-DACH, as compared to that of two ammines, could make the difference and be responsible for the markedly lowered tolerance of DNA adducts formed by **1**.

CONCLUSIONS

Although the encouraging antitumor activity of [$PtCl_2$(*cis*-1,4-DACH)] was shown in early studies almost 20 years ago, the compound has remained nearly neglected. By extending the investigation to human chemotherapy-resistant cancer cells, we have demonstrated the real effectiveness of **1** in circumventing cisplatin and oxaliplatin resistance. Moreover, **1** has been found not to be a P-gp substrate, being active against colon MDR cells, and to completely circumvent oxaliplatin resistance in LoVo colon cancer cells. The uptake of compound **1** by the latter cells was similar to that of sensitive LoVo cells. This is not the case for all other compounds considered in this investigation. Therefore, somehow compound **1** can escape the decreased uptake and/or increased export mechanisms typical of resistant cells. Moreover, as found in a previous investigation, the DNA adducts of **1** are removed from repair systems with lower efficiency than the adducts of cisplatin and are more effective in inhibiting DNA and RNA polymerase.

At the moment, interaction with ds-DNA investigated by a biosensor assay and QM/MM geometry optimization of the 1,2-GG intrastrand cross-links have failed to show significant differences between DNA adducts of **1** and **2** (the latter mimicking oxaliplatin). However, there is some evidence that **1** induces different distortions in DNA compared to **2** and that it may be more like cisplatin than oxaliplatin, but this needs further investigations to be confirmed.

In conclusion, the unique antitumor effects of **1**, coupled with its enhanced aqueous solubility compared to that of **2**, make this compound a potential "magic bullet" against oxaliplatin-resistant colorectal cancer cells, and its evaluation in clinical studies is highly desirable, despite the fringe market that this drug could find.

As a further step in the elucidation of the different anticancer activity of [$PtCl_2$(*cis*-1,4-DACH)], as compared to cisplatin and oxaliplatin, we intend to investigate the structural distortions induced by [$PtCl_2$(*cis*-1,4-DACH)] in longer DNA duplexes and the cellular processing of these DNA lesions, comprising real-time polymerase chain reaction (PCR) and Western blot analysis, to measure the level of expression of key proteins mediating the antitumor activity of platinum drugs.

As a final remark, we suggest for [$PtCl_2$(*cis*-1,4-DACH)] the nickname "kiteplatin" on the basis of its structural features[15] resembling a parachute (the *cis*-1,4-DACH ligand) on a skydiver (the metal).

EXPERIMENTAL SECTION

Chemicals. Commercial reagents (1(*R*),2(*R*)-diaminocyclohexane, $AgNO_3$, KI, KCl, etc.), solvents, MTT, cisplatin, and oxaliplatin were

dx.doi.org/10.1021/jm3006838 | J. Med. Chem. 2012, 55, 7182−7192

purchased from Sigma Chemical Co. (St. Louis, MO) and used as received.

[$PtCl_2$(*cis*-1,4-DACH)], **1**, was prepared as described previously.[15] [$PtCl_2$(1(*R*),2(*R*)-DACH)], **2**, was prepared according to the method of Dhara.[46] Briefly, $K_2[PtCl_4]$ (0.726 g, 1.75 mmol) was dissolved in a minimum amount of water (15 mL), and the resulting red solution was treated with KI (1.74 g, 10.5 mmol). After being stirred for 5 min, the brown solution was treated with 1(*R*),2(*R*)-diaminocyclohexane (200 mg, 1.75 mmol), which caused the immediate formation of a yellow precipitate. The suspension was stirred for 3 h. The yellow precipitate, [PtI_2(1(*R*),2(*R*)-DACH)], was then collected by filtration, washed with water, ethanol, and diethyl ether, dried under vacuum, and analyzed by elemental analysis. A yield of 1.36 g (91%) was obtained. [PtI_2(1(*R*),2(*R*)-DACH)] (182 mg, 0.32 mmol) was then suspended in 20 mL of water and treated with $AgNO_3$ (109 mg, 0.64 mmol), which caused the immediate formation of a yellow precipitate (AgI). The suspension was kept at 55 °C in the dark for 30 min, AgI was separated by filtration of the mother liquor through Celite, and the filtrate was treated with KCl (1.43 g, 1.92 mmol). The obtained solution was stirred at 55 °C for 30 min, resulting in the formation of a yellow precipitate. The yellow precipitate, corresponding to **2**, was isolated by filtration, washed with ice-cold water, ethanol, and ether, and then dried under vacuum. A yield of 0.30 g (94%) was obtained. The elemental analyses and the spectroscopic and spectrometric properties of the synthesized Pt complexes were consistent with the data reported in the literature.[15,47] The purity of the synthesized compounds was higher than 95% as established by combustion analysis.

Cell Cultures. Human breast (MCF-7) and colon (HCT-15 and LoVo) carcinoma cell lines along with melanoma (A375) were obtained from the American Type Culture Collection (ATCC, Rockville, MD). A431 cells are human cervical carcinoma cells kindly provided by Prof. F. Zunino (Molecular Pharmacology Unit, Experimental Oncology and Molecular Medicine, Istituto Nazionale dei Tumori, Milan, Italy). 2008 and its cisplatin resistant variant, C13*, are human ovarian cancer cell lines kindly provided by Prof. G. Marverti (Department of Biomedical Science, University of Modena, Italy). The LoVo-OXP cells were derived using a standard protocol in which LoVo cells were grown in increasing concentrations of oxaliplatin and resistant clones were selected over a period of nine months.[48]

Cell lines were maintained in the logarithmic phase at 37 °C in a 5% carbon dioxide atmosphere using the following culture media containing 10% fetal calf serum (Euroclone, Milan, Italy), antibiotics (50 units mL^{-1} penicillin and 50 mg mL^{-1} streptomycin), and 2 mM L-glutamine: (i) RPMI-1640 medium (Euroclone) for MCF-7, HCT-15, A431, 2008, and C13* cells, (ii) Ham's F-12 medium (Sigma Chemical Co.) for LoVo, LoVo MDR, and LoVo-OXP cells, and (iii) Dulbecco's modified Eagle's medium (DMEM) for A375 cells.

Cytotoxicity Assay. The growth inhibitory effect toward tumor cell lines was evaluated by means of the MTT assay.[49] Briefly, depending upon the growth characteristics of the cell line, (3−8) × 10^3 cells $well^{-1}$, were seeded in 96-well microplates in growth medium (100 μL) and then incubated at 37 °C in a 5% carbon dioxide atmosphere. After 24 h, the medium was removed and replaced with a fresh one containing the compound to be studied, at the appropriate concentration, dissolved in 0.9% sodium chloride solution just before use. Triplicate cultures were established for each treatment. After 72 h, each well was treated with 10 μL of a 5 mg mL^{-1} MTT saline solution, and after 5 h of incubation, 100 μL of a sodium dodecyl sulfate (SDS) solution in 0.01 M HCl was added. After an overnight incubation, the inhibition of cell growth induced by the tested complexes was determined by measuring the absorbance of each well at 570 nm using a Bio-Rad 680 microplate reader. The mean absorbance for each drug dose was expressed as a percentage of the control and plotted vs drug concentration. Dose−response curves were fitted, and IC_{50} values were calculated with the four-parameter logistic model (4PL). IC_{50} values represent the drug concentrations that reduce the mean absorbance at 570 nm to 50% of that in the untreated control wells.

Cellular Uptake. LoVo and LoVo-OXP cells (2×10^6) were seeded in 75 cm^2 flasks in growth medium (20 mL). After 24 h, the medium was replaced, and the cells were incubated for different times (6, 24, or 48 h) in the presence of the tested complexes. Cell monolayers were washed twice with cold PBS and harvested. Samples were subjected to three freezing/thawing cycles at −80 °C and then vigorously vortexed. Aliquots were removed for the determination of protein content by the BioRad protein assay (BioRad). The samples were treated with 1 mL of highly pure nitric acid ([Pt] ≤ 0.01 μg kg^{-1}, TraceSELECT Ultra, Sigma Chemical Co.) and transferred into a microwave Teflon vessel. Subsequently, samples were submitted to the standard procedure using a speed wave MWS-3 Berghof instrument (Eningen, Germany). After cooling, each mineralized sample was analyzed for platinum by using a Varian AA Duo graphite furnace atomic absorption spectrometer (Varian, Palo Alto, CA) at a wavelength of 324.7 nm. The calibration curve was obtained using known concentrations of standard solutions purchased from Sigma Chemical Co.

Determination of the Partition Coefficient log $P_{o/w}$. Chromatographic analysis was used to evaluate the partition coefficient of **1**. The chromatographic conditions were[33] silica-based C18 gel as the stationary phase (5 μm Phenomenex Gemini C18 column, 25 × 3 mm i.d.) and mobile phase containing different percentages of a 15 mM water solution of HCOOH and MeOH (flow rate 0.75 mL min^{-1}, isocratic elution, UV−vis detector set at 210 nm). KCl was used as the internal reference to determine the column dead time (t_0).[50] The platinum complex solutions were 0.25 mM. A chromatographic run was performed with every different eluent composition (the methanol fraction ranging from 20% to 50%, v/v), and the corresponding retention time t_R was used to calculate log k' ($k' = (t_R - t_0)/t_0$).

Starting from these data, the log k' to 0% MeOH (log k'_0), corresponding to the capacity factor in pure water, was extrapolated.[51] The log k'_0 values of compounds with known log $P_{o/w}$ values were used to generate the calibration curve necessary to predict the unknown log $P_{o/w}$ of **1**.[33]

In Vivo Anticancer Activity toward Lewis Lung Carcinoma. All studies involving animal testing were carried out in accordance with the ethical guidelines for animal research adopted by the University of Padua, acknowledging the Italian regulation and European Directive 86/609/EEC as to the animal welfare and protection and the related codes of practice. The mice were purchased by Charles River, Italy, housed in steel cages under controlled environmental conditions (constant temperature, humidity, and 12 h dark/light cycle), and alimented with commercial standard feed and tap water ad libitum. Animals were observed daily and body weight and food intake recorded. The LLC cell line was purchased from ECACC, United Kingdom. The LLC cell line was maintained in DMEM (Euroclone) supplemented with 10% heat-inactivated fetal bovine serum (FBS; Euroclone), 10 mM L-glutamine, 100 U mL^{-1} penicillin, and 100 μg mL^{-1} streptomycin in a 5% CO_2 air incubator at 37 °C.

The LLC was implanted intramuscularly (im) as a 2×10^6 cell inoculum into the right hind leg of 8 week old male and female C57BL mice (24 ± 3 g body weight). After 24 h from tumor implantation, mice were randomly divided into five groups (8 animals per group, 10 controls) and treated with a daily ip injection of **1** (1.5 and 3 mg kg^{-1} in 0.9% NaCl solution), cisplatin (1.5 mg kg^{-1} in 0.9% NaCl solution), or the vehicle solution (0.9% NaCl solution) from day 9 after tumor inoculation (palpable tumor). At day 15, animals were sacrificed, the legs were amputated at the proximal end of the femur, and the inhibition of tumor growth was determined according to the difference in weight of the tumor-bearing leg and the healthy leg of the animals expressed as a percentage referred to the control animals. Body weight was measured every two days and was taken as a parameter for systemic toxicity.

All the values are the means ± SD of not less than three measurements. Multiple comparisons were made by the Tukey−Kramer test (**, $p < 0.01$; * or ○, $p < 0.05$).

Interaction between Platinum Complexes and DNA Biosensors. The DNA biosensor was prepared as previously described.[35] Briefly, the planar, disposable, screen-printed electrochemical cell

(SPE) consisted of a graphite working electrode, a graphite counter electrode, and a silver pseudoreference electrode. The electrode surface was activated by applying a potential of +1.6 V for 2 min and +1.8 V for 1 min in 0.25 M acetic acid buffer (pH 4.75) containing 10 mM KCl. After this pretreatment, ds-DNA was immobilized at a fixed potential (+0.5 V versus Ag pseudoreference electrode for 300 s) onto the SPE surface by dipping the strip into the test solution containing ds-DNA and platinum drug (sample test) or ds-DNA only (blank test). The sensor was then immersed in acetate buffer, and an SWV scan was carried out to measure the oxidation peak height (at +0.95 V versus Ag pseudoreference electrode) of unplatinated guanine residues present in the DNA attached to the electrode surface. Interaction of the platinum drugs with DNA was evaluated by changes in the magnitude of the oxidation peak for guanine adsorbed onto the SPE, i.e., the ratio (%) between the guanine peak height of the platinated DNA (S_{sample}) and that of the DNA in the buffer solution without drug (S_{blank}) (S (%) = (S_{sample}/S_{blank}) × 100). Analyte solutions of the platinum drugs (0.25 mM) were prepared in 50 mM phosphate buffer (PB), 5 mM NaCl (pH 7.0), and 2% v/v DMSO. After addition of the ds-DNA to the solutions (DNA final concentration 50 ppm), the resulting mixtures were gently stirred at 25 °C, and at various times the electrochemical activity of the G residues on DNA was sampled with the sensor.

Conductivity Measurements. The experiments were performed using an Orion 120 conductivity meter in DMSO at 25 ± 0.1 °C using a thermostatic circulating bath to keep constant the temperature of the sample. The analyses were carried out on freshly prepared solutions of the complexes in DMSO (0.5 mM) by measuring conductivity at regular time intervals over 24 h.

Computational Methods. Atomic coordinates of an oxaliplatin–DNA complex were extracted from PDB entry 1PGC,[42] and truncated to a GG/CC base-pair step plus drug. From these coordinates, 1(*R*),2(*R*)-diaminocyclohexane was mutated into *cis*-1,4-diaminocyclohexane by hand, retaining the position of the platinum and coordinated nitrogen atoms and adopting a boatlike conformation for cyclohexane. These coordinates were used to set up QM/MM ONIOM calculations,[52] in which Pt, diaminocyclohexane, and two guanine moieties were treated with DFT and the remaining atoms with the AMBER94[53] force field as defined within GAUSSIAN 03.[54] The DFT functional employed was Becke's half-and-half method,[55] previously shown to give an acceptable description of the DNA structure and π-stacking,[56] with the 6-31+G(d,p) basis set on all light atoms and SDD basis set and ECP on Pt. Hydrogen atoms were used to terminate the QM region at the N9—C1′ bond, as shown in Figure 6. AMBER atom types and charges in the MM region were assigned in GausView where possible and checked by hand, while atomic charges in the QM region were calculated using the procedure of Merz and Kollman.[57]

Geometry optimization of each structure then proceeded in three stages using GAUSSIAN 03. Initially, all atoms in the MM layer were held fixed while all QM atoms, except the hydrogen link atoms, were optimized. Then QM atoms were fixed and all MM atoms optimized. Finally, full optimization of the geometry of all atoms was performed in Cartesian coordinates.

The resulting geometries were used to calculate binding energies of the platinum drugs to DNA using several theoretical methods. First, the same scheme as used for geometry optimization was employed, in which the platinum fragment was treated with DFT while the DNA fragment was treated with QM/MM, with guanines in the QM region and all other atoms in MM. Second, DFT description of all atoms used Grimme's B97-D functional[58] with the def2-TZVP basis set, employing resolution of identity (RI) approximation in Turbomole version 5.10.[59] Finally, the binding energy was calculated using the PM6-DH2 semiempirical method[60,61] and the MOPAC package.[62] PM6 is a reparametrization of the popular PM3 method that includes Pt, while "DH2" is an empirical correction scheme that accounts for the known shortcomings of all semiempirical methods for noncovalent interactions such as hydrogen bonding and π-stacking. In all cases, the binding energy was calculated at the adduct geometry, i.e., no relaxation of DNA or platinum fragment was taken into account, following previous work in our group on a series of Pt(en) complexes.[63] Counterpoise corrections to binding energy were found to be less than 1 kcal mol^{-1} and were not employed. The effect of aqueous solvation on binding energies was estimated using the conductor-like screening (COSMO) approach.[64] The QM/MM-optimized geometries were also used to analyze DNA structures via the X3DNA suite of programs.[65]

Exactly the same procedure was followed from PDB entry 1IHH,[43] which led to an essentially identical final geometry (see the Supporting Information).

■ ASSOCIATED CONTENT

Ⓢ Supporting Information

Comparison of selected angles and distances from the QM/MM geometry-optimized 1,2-GG intrastrand cross-links, formed by **1** and **2**, obtained starting from PDB entries 1PGC (ref 42) and 1IHH (ref 43). This material is available free of charge via the Internet at http://pubs.acs.org.

■ AUTHOR INFORMATION

Corresponding Author

*Phone: +39-080-5442759 (N.M.); +39-080-5442774 (G.N.). Fax: +39-080-5442230 (N.M.); +39-080-5442230 (G.N.). E-mail: nicola.margiotta@uniba.it (N.M.); giovanni.natile@uniba.it (G.N.).

Notes

The authors declare no competing financial interest.

■ ACKNOWLEDGMENTS

We thank the University of Bari (Fondi di Ateneo), the Italian "Ministero dell'Università e della Ricerca" (PRIN2009 n. 2009WCNS5C_004), the European Commission (EC) (European Cooperation in Science and Technology (COST) Action CM1105), and the Inter-University Consortium for Research on the Chemistry of Metal Ions in Biological Systems (CIRCMSB, Bari, Italy) for support. J.A.P. thanks the Leverhulme Trust for a research fellowship.

■ ABBREVIATIONS USED

DACH, diaminocyclohexane; DMSO, dimethyl sulfoxide; GF-AAS, graphite furnace atomic absorption analysis; HH, head-to-head; HT, head-to-tail; IC_{50}, half-maximum inhibitory concentration; MRD, multi-drug-resistant; MRP, multi-drug-resistance protein; NER, nucleotide excision repair; PBS, phosphate-buffered saline; P-gp, P-glycoprotein; RF, resistance factor; QM/MM, quantum mechanics/molecular mechanics; RP-HPLC, reversed-phase high-pressure liquid chromatography; SD, standard deviation; SPE, screen-printed electrode; SWV, square wave voltammetry

■ REFERENCES

(1) *Cisplatin: Chemistry and Biochemistry of a Leading Anticancer Drug*; Lippert, B., Ed.; Verlag Helvetica Chimica Acta: Zürich, Switzerland, 2000; 563 pp.

(2) Jakupec, M. A.; Galanski, M.; Arion, V. B.; Hartinger, C. G.; Keppler, B. K. Antitumour metal compounds: more than theme and variations. *Dalton Trans.* **2008**, 183–194.

(3) Kelland, L. The resurgence of platinum-based cancer chemotherapy. *Nat. Rev. Cancer* **2007**, *7*, 573–584.

(4) Reedijk, J. Platinum anticancer coordination compounds: study of DNA binding inspires new drug design. *Eur. J. Inorg. Chem.* **2009**, 1303–1312.

(5) Wong, E.; Giandomenico, C. M. Current status of platinum-based antitumor drugs. *Chem. Rev.* **1999**, *99*, 2451–2466.

(6) Hall, M. D.; Mellor, H. R.; Callaghan, R.; Hambley, T. W. Basis for design and development of platinum(IV) anticancer complexes. *J. Med. Chem.* **2007**, *50*, 3403−3411.
(7) Wheate, N. J.; Walker, S.; Craig, G. E.; Oun, R. The status of platinum anticancer drugs in the clinic and in clinical trials. *Dalton Trans.* **2010**, *39*, 8113−8127.
(8) Hoeschele, J. D.; Hollis Showalter, H. D.; Kraker, A. J.; Elliott, W. L.; Roberts, B. J.; Kampf, J. W. Synthesis, structural characterization, and antitumor properties of a novel class of large-ring platinum(II) chelate complexes incorporating the *cis*-1,4-diaminocyclohexane ligand in a unique locked boat conformation. *J. Med. Chem.* **1994**, *37*, 2630−2636.
(9) Shamsuddin, S.; Takahashi, I.; Siddik, Z. H.; Khokhar, A. R. Synthesis, characterization, and antitumor activity of a series of novel cisplatin analogs with *cis*-1,4-diaminocyclohexane as nonleaving amine group. *J. Inorg. Biochem.* **1996**, *61*, 291−301.
(10) Shamsuddin, S.; Santillan, C. C.; Stark, J. L.; Whitmire, K. H.; Siddik, Z. H.; Khokhar, A. R. Synthesis, characterization, and antitumor activity of new platinum(IV) trans-carboxylate complexes: crystal structure of [Pt(*cis*-1,4-DACH) *trans*-$(acetate)_2Cl_2$]. *J. Inorg. Biochem.* **1998**, *71*, 29−35.
(11) Ali, M. S.; Khokhar, A. R. *cis*-1,4-Diaminocyclohexane-Pt(II) and -(IV) adducts with DNA bases and nucleosides. *J. Inorg. Biochem.* **2003**, *96*, 452−456.
(12) Shamsuddin, S.; Ali, M. S.; Whitmire, K. H.; Khokhar, A. R. Synthesis characterization and X-ray crystal structures of *cis*-1,4-diaminocyclohexane-platinum(II) nucleobase adducts. *Polyhedron* **2007**, *26*, 637−644.
(13) Wang, D.; Lippard, S. J. Cellular processing of platinum anticancer drugs. *Nat. Rev. Drug Discovery* **2005**, *4*, 307−320.
(14) Fuertes, M. A.; Alonso, C.; Pérez, J. M. Biochemical modulation of cisplatin mechanisms of action: enhancement of antitumor activity and circumvention of drug resistance. *Chem. Rev.* **2003**, *103*, 645−662.
(15) Ranaldo, R.; Margiotta, N.; Intini, F. P.; Pacifico, C.; Natile, G. Conformer distribution in (*cis*-1,4-DACH)bis(guanosine-5′-phosphate)platinum(II) adducts: a reliable model for DNA adducts of antitumoral cisplatin. *Inorg. Chem.* **2008**, *47*, 2820−2830.
(16) Natile, G.; Marzilli, L. G. Non-covalent interactions in adducts of platinum drugs with nucleobases in nucleotides and DNA as revealed by using chiral substrates. *Coord. Chem. Rev.* **2006**, *250*, 1315−1331 and references therein.
(17) Kasparkova, J.; Suchankova, T.; Halamikova, A.; Zerzankova, L.; Vrana, O.; Margiotta, N.; Natile, G.; Brabec, V. Cytotoxicity, cellular uptake, glutathione and DNA interactions of an antitumor large-ring Pt(II) chelate complex incorporating the *cis*-1,4-diaminocyclohexane carrier ligand. *Biochem. Pharmacol.* **2010**, *79*, 552−564.
(18) Van Cutsem, E.; Peeters, M.; Siena, S.; Humblet, Y.; Hendlisz, A.; Neyns, B.; Canon, J.-L.; Van Laethem, J.-L.; Maurel, J.; Richardson, G.; Wolf, M.; Amado, R. G. Open-label phase III trial of panitumumab plus best supportive care compared with best supportive care alone in patients with chemotherapy-refractory metastatic colorectal cancer. *J. Clin. Oncol.* **2007**, *25*, 1658−1664.
(19) Saltz, L. B.; Meropol, N. J.; Loehrer, P. J., Sr; Needle, M. N.; Kopit, J.; Mayer, R. J. Phase II trial of cetuximab in patients with refractory colorectal cancer that expresses the epidermal growth factor receptor. *J. Clin. Oncol.* **2004**, *22*, 1201−1208.
(20) Sobrero, A. F.; Maurel, J.; Fehrenbacher, L.; Scheithauer, W.; Abubakr, Y. A.; Lutz, M. P.; Vega-Villegas, M. E.; Eng, C.; Steinhauer, E. U.; Prausova, J.; Lenz, H.-J.; Borg, C.; Middleton, G.; Kröning, H.; Luppi, G.; Kisker, O.; Zubel, A.; Langer, C.; Kopit, J.; Burris, H. A., III. EPIC: phase III trial of cetuximab plus irinotecan after fluoropyrimidine and oxaliplatin failure in patients with metastatic colorectal cancer. *J. Clin. Oncol.* **2008**, *26*, 2311−2319.
(21) Eastman, A. The formation, isolation and characterization of DNA adducts produced by anticancer platinum complexes. *Pharmacol. Ther.* **1987**, *34*, 155−166.
(22) Woynarowski, J. M.; Chapman, W. G.; Napier, C.; Herzig, M. C. S.; Juniewicz, P. Sequence- and region-specificity of oxaliplatin adducts in naked and cellular DNA. *Mol. Pharmacol.* **1998**, *54*, 770−777.
(23) Zhou, Y.; Ling, X. L.; Li, S. W.; Li, X. Q.; Yan, B. Establishment of a human hepatoma multidrug resistant cell line in vitro. *World J. Gastroenterol.* **2010**, *16*, 2291−2297.
(24) Kamazawa, S.; Kigawa, J.; Kanamori, Y.; Itamochi, H.; Sato, S.; Iba, T.; Terakawa, N. Multidrug resistance gene-1 is a useful predictor of paclitaxel-based chemotherapy for patients with ovarian cancer. *Gynecol. Oncol.* **2002**, *86*, 171−176.
(25) Zhang, Y. H.; Wu, Q.; Xiao, X. Y.; Li, D. W.; Wang, X. P. Silencing MRP4 by small interfering RNA reverses acquired DDP resistance of gastric cancer cell. *Cancer Lett.* **2010**, *291*, 76−82.
(26) Noordhuis, P.; Laan, A. C.; van de Born, K.; Losekoot, N.; Kathmann, I.; Peters, G. J. Oxaliplatin activity in selected and unselected human ovarian and colorectal cancer cell lines. *Biochem. Pharmacol.* **2008**, *76*, 53−61.
(27) Gatti, L.; Perego, P. Cellular resistance to oxaliplatin and drug accumulation defects. In *Cancer Drug Discovery and Development: Platinum and Other Heavy Metal Compounds in Cancer Chemotherapy*; Bonetti, A., Leone, R., Muggia, F., Howell, S. B., Eds.; Humana Press: New York, 2009; pp 115−124.
(28) Wersinger, C.; Rebel, G.; Lelong-Rebel, I. H. Detailed study of the different taurine uptake systems of colon LoVo MDR and non-MDR cell lines. *Amino Acids* **2000**, *19*, 667−685.
(29) Abramkin, S. A.; Jungwirth, U.; Valiahdi, S. M.; Dworak, C.; Habala, L.; Meelich, K.; Berger, W.; Jakupec, M. A.; Hartinger, C. G.; Nazarov, A. A.; Galanski, M.; Keppler, B. K. {(1*R*,2*R*,4*R*)-4-Methyl-1,2-cyclohexanediamine}oxalatoplatinum(II): a novel enantiomerically pure oxaliplatin derivative showing improved anticancer activity in vivo. *J. Med. Chem.* **2010**, *53*, 7356−7364.
(30) Platts, J. A.; Hibbs, D. E.; Hambley, T. W.; Hall, M. D. Calculation of the hydrophobicity of platinum drugs. *J. Med. Chem.* **2001**, *44*, 472−474.
(31) Ghezzi, A. R.; Aceto, M.; Cassino, C.; Gabano, E.; Osella, D. Uptake of antitumor platinum(II)-complexes by cancer cells, assayed by inductively coupled plasma mass spectrometry (ICP-MS). *J. Inorg. Biochem.* **2004**, *98*, 73−78.
(32) Liu, X.; Testa, B.; Fahr, A. Lipophilicity and its relationship with passive drug permeation. *Pharm. Res.* **2011**, *28*, 962−977.
(33) Platts, J. A.; Oldfield, S. P.; Reif, M. M.; Palmucci, A.; Gabano, E.; Osella, D. The RP-HPLC measurement and QSPR analysis of logPo/w values of several Pt(II) complexes. *J. Inorg. Biochem.* **2006**, *100*, 1199−1207.
(34) Bagni, G.; Osella, D.; Sturchio, E.; Mascini, M. Deoxyribonucleic acid (DNA) biosensors for environmental risk assessment and drug studies. *Anal. Chim. Acta* **2006**, *573*−*574*, 81−89.
(35) Ravera, M.; Bagni, G.; Mascini, M.; Dabrowiak, J. C.; Osella, D. The activation of platinum(II) antiproliferative drugs in carbonate medium evaluated by means of a DNA-biosensor. *J. Inorg. Biochem.* **2007**, *101*, 1023−1027.
(36) Ravera, M.; Baracco, S.; Cassino, C.; Colangelo, D.; Bagni, G.; Sava, G.; Osella, D. Electrochemical measurements confirm the preferential bonding of the antimetastatic complex [ImH]-[$RuCl_4$(DSMO)(Im)] (NAMI-A) with the proteins and the weak interaction with nucleobases. *J. Inorg. Biochem.* **2004**, *98*, 984−990.
(37) Bagni, G.; Ravera, M.; Osella, D.; Mascini, M. Electrochemical biosensors as a screening tool of in vitro DNA-drug interaction. *Curr. Pharm. Anal.* **2005**, *1*, 217−224.
(38) Mascini, M.; Bagni, G.; Di Pietro, M. L.; Ravera, M.; Baracco, S.; Osella, D. Electrochemical biosensor evaluation of the interaction between DNA and metallo-drugs. *BioMetals* **2006**, *19*, 409−418.
(39) Ravera, M.; Bagni, G.; Mascini, M.; Osella, D. DNA-metallodrugs interactions signaled by electrochemical biosensors: an overview. *Bioinorg. Chem. Appl.* **2007**, No. 91078.
(40) Geary, W. J. The use of conductivity measurements in organic solvents for the characterisation of coordination compounds. *Coord. Chem. Rev.* **1971**, *7*, 81−122.
(41) Wilkins, R. G. *Kinetics and Mechanism of Reactions of Transition Metal Complexes*, 2nd ed.; Wiley-VCH: Weinheim, Germany, 2002; Chapter 3.10.3.

(42) Wu, Y.; Pradhan, P.; Havener, J.; Boysen, G.; Swenberg, J. A.; Campbell, S. L.; Chaney, S. G. NMR solution structure of an oxaliplatin 1,2-d(GG) intrastrand cross-link in a DNA dodecamer duplex. *J. Mol. Biol.* **2004**, *341*, 1251−1269.
(43) Spingler, B.; Whittington, D. A.; Lippard, S. J. 2.4 Å crystal structure of an oxaliplatin 1,2-d(GpG) intrastrand cross-link in a DNA dodecamer duplex. *Inorg. Chem.* **2001**, *40*, 5596−5602.
(44) Mutter, S. T.; Platts, J. A. Unpublished results.
(45) Brabec, V.; Malina, J.; Margiotta, N.; Natile, G.; Kasparkova, J. Unpublished results.
(46) Dhara, S. C. A rapid method for the synthesis of *cis*-$[Pt(NH_3)_2Cl_2]$. *Indian J. Chem.* **1970**, *8*, 193−194.
(47) Kidani, Y.; Inagaki, K. Antitumor activity of 1,2-diaminocyclohexane-platinum complexes against sarcoma-180 ascites form. *J. Med. Chem.* **1978**, *21*, 1315−1318.
(48) Gandin, V.; Pellei, M.; Tisato, F.; Porchia, M.; Santini, C.; Marzano, C. A novel copper complex induces paraptosis in colon cancer cells via the activation of ER stress signalling. *J. Cell. Mol. Med.* **2012**, *16*, 142−151.
(49) Alley, M. C.; Scudiero, D. A.; Monks, A.; Hursey, M. L.; Czerwinski, M. J.; Fine, D. L.; Abbott, B. J.; Mayo, J. G.; Shoemaker, R. H.; Boyd, M. R. Feasibility of drug screening with panels of human tumor cell lines using a microculture tetrazolium assay. *Cancer Res.* **1988**, *48*, 589−601.
(50) Heudi, O.; Mercier−Jobard, S.; Cailleux, A.; Allain, P. Mechanisms of reaction of L-methionine with carboplatin and oxaliplatin in different media: a comparison with cisplatin. *Biopharm. Drug Dispos.* **1999**, *20*, 107−116.
(51) Valkó, K.; Snyder, L. R.; Glajch, J. L. Retention in reversed-phase liquid-chromatography as a function of mobile-phase composition. *J. Chromatogr., A* **1993**, *656*, 501−520.
(52) Vreven, T.; Byun, K. S.; Komáromi, I.; Dapprich, S.; Montgomery, J. A., Jr.; Morokuma, K.; Frisch, M. J. Combining quantum mechanics methods with molecular mechanics methods in ONIOM. *J. Chem. Theory Comput.* **2006**, *2*, 815−826.
(53) Cornell, W. D.; Cieplak, P.; Bayly, C. I.; Gould, I. R.; Merz, K. M., Jr.; Ferguson, D. M.; Spellmeyer, D. C.; Fox, T.; Caldwell, J. W.; Kollman, P. A. A second generation force-field for the simulation of proteins, nucleic-acids, and organic-molecules. *J. Am. Chem. Soc.* **1995**, *117*, 5179−5197.
(54) Frisch, M. J.; Trucks, G. W.; Schlegel, H. B.; Scuseria, G. E.; Robb, M. A.; Cheeseman, J. R.; Montgomery, J. A. Jr.; Vreven, T.; Kudin, K. N.; Burant, J. C.; Millam, J. M.; Iyengar, S. S.; Tomasi, J.; Barone, V.; Mennucci, B.; Cossi, M.; Scalmani, G.; Rega, N.; Petersson, G. A.; Nakatsuji, H.; Hada, M.; Ehara, M.; Toyota, K.; Fukuda, R.; Hasegawa, J.; Ishida, M.; Nakajima, T.; Honda, Y.; Kitao, O.; Nakai, H.; Klene, M.; Li, X.; Knox, J. E.; Hratchian, H. P.; Cross, J. B.; Bakken, V.; Adamo, C.; Jaramillo, J.; Gomperts, R.; Stratmann, R. E.; Yazyev, O.; Austin, A. J.; Cammi, R.; Pomelli, C.; Ochterski, J.; Ayala, P. Y.; Morokuma, K.; Voth, G. A.; Salvador, P.; Dannenberg, J. J.; Zakrzewski, V. G.; Dapprich, S.; Daniels, A. D.; Strain, M. C.; Farkas, O.; Malick, D. K.; Rabuck, A. D.; Raghavachari, K.; Foresman, J. B.; Ortiz, J. V.; Cui, Q.; Baboul, A. G.; Clifford, S.; Cioslowski, J.; Stefanov, B. B.; Liu, G.; Liashenko, A.; Piskorz, P.; Komaromi, I.; Martin, R. L.; Fox, D. J.; Keith, T.; Al-Laham, M. A.; Peng, C. Y.; Nanayakkara, A.; Challacombe, M.; Gill, P. M. W.; Johnson, B. G.; Chen, W.; Wong, M. W.; Gonzalez, C.; Pople, J. A. *GAUSSIAN 03*, revision E.01; Gaussian, Inc.: Wallingford, CT, 2004.
(55) Becke, A. D. A new mixing of Hartree-Fock and local density-functional theories. *J. Chem. Phys.* **1993**, *98*, 1372−1377.
(56) Waller, M. P.; Robertazzi, A.; Platts, J. A.; Hibbs, D. E.; Williams, P. A. Hybrid density functional π-stacking interactions: application to benzenes, pyridines, and theory for DNA bases. *J. Comput. Chem.* **2006**, *27*, 491−504.
(57) Singh, U. C.; Kollman, P. A. An approach to computing electrostatic charges for molecules. *J. Comput. Chem.* **1984**, *5*, 129−145.
(58) Grimme, S. Semiempirical GGA-type density functional constructed with a long-range dispersion correction. *J. Comput. Chem.* **2006**, *27*, 1787−1799.
(59) Ahlrichs, R.; Bar, M.; Haser, M.; Horn, H.; Kolmel, C. Electronic structure calculations on workstation computers: the program system turbomole. *Chem. Phys. Lett.* **1989**, *162*, 165−169.
(60) Stewart, J. J. P. Optimization of parameters for semiempirical methods V: modification of NDDO approximations and application to 70 elements. *J. Mol. Model.* **2007**, *13*, 1173−1213.
(61) Korth, M.; Pitonak, M.; Rezac, J.; Hobza, P. A transferable H-bonding correction for semiempirical quantum-chemical methods. *J. Chem. Theory Comput.* **2010**, *6*, 344−352.
(62) Stewart, J. J. P. MOPAC, 2009. http://openMOPAC.net (Accessed February 2, 2012).
(63) Gkionis, K.; Platts, J. A. QM/MM investigation into binding of square-planar platinum complexes to DNA fragments. *J. Biol. Inorg. Chem.* **2009**, *14*, 1165−1174.
(64) Klamt, A.; Schüürmann, G. COSMO: a new approach to dielectric screening in solvents with explicit expressions for the screening energy and its gradient. *J. Chem. Soc., Perkin Trans.* **1993**, *2*, 799−805.
(65) Lu, X.-J.; Olson, W. K. 3DNA: a software package for the analysis, rebuilding and visualization of three-dimensional nucleic acid structures. *Nucleic Acids Res.* **2003**, *31*, 5108−5121.